



Uplift of an Underground Tank in Northern Malabar Region, India

Nilesh P. Shirode, Head - Civil Dept., Toyo Engineering India Pvt. Ltd., Mumbai, India; email: nilesh.shirode@toyo-eng.com

Kedar C. Birid, Asst. Manager, Toyo Engineering India Pvt. Ltd., Mumbai, India; email: kedar.birid@toyo-eng.com

S. R. Gandhi, Director, Sardar Vallabhbhai National Institute of Technology, Surat, India; email: srgandhi@gmail.com

Rajesh Nair, Associate Professor of Petroleum Engineering, Dept. of Ocean Engineering, IIT Madras, India; email: rajeshnair@iitm.ac.in

ABSTRACT: An underground reinforced concrete tank was constructed for a project in the southwest region of India. The tank was 90 m x 35 m in plan and 7.3 m deep resting on partly filled-up and partly native soil. During the peak monsoon, a sudden uplifting of the base slab by about 300 mm and subsequent failure of the foundation raft and a partition wall was observed. Laboratory testing was executed and hydrogeological survey was carried out using ground penetrating radar, seismic refraction and infiltrometer testing, and an analytical study was carried out to identify the root cause of the tank uplifting. Based on this study, it was observed that the uplifting and structural failure was essentially due to the peculiar land terrain and soil properties and the development of excess hydraulic head below the bottom of the tank. After considering different options, the rectification measures were carried out by provision of dewatering wells along the tank periphery to release the excess hydrostatic pressure and stabilize the foundation raft. The structural repair of the top of the foundation raft and partition wall was carried out to strengthen the reinforced concrete members. The rectification measures worked well to increase the structural stability of the tank and to prevent build-up of excess hydrostatic pressure preventing uplift and subsequent damage in the future.

KEYWORDS: uplifting, hydrogeological survey, hydrostatic pressure, ground penetrating radar, seismic refraction

SITE LOCATION: [Geo-Database](#)

INTRODUCTION

An underground reinforced concrete tank was under construction to receive contaminated rainwater from nearby areas within a plant at Mangalore city in Karnataka state of India. The topography of the original land was highly undulating and involved extensive cutting and filling works to level the ground. The tank under study was located within the filled up soil. The southwest region of India is characterized by heavy rainfall during the monsoon season leading to a rise in groundwater table. During heavy rains, when the tank was partly constructed, a sudden uplifting of the foundation raft was observed. Though the immediate root cause for such a failure was speculated to be due to the excess hydrostatic pressure beneath the tank, a detailed hydrogeological survey was planned to determine the appropriate rectification measures.

DETAILS OF THE UNDERGROUND TANK

The underground reinforced concrete tank, which was under construction, got uplifted in mid-June of 2013. During uplifting, the tank raft foundation and four side walls of the tank were completed. The purpose of this tank was to collect the contaminated rainwater from the plant area and store it temporarily before it is sent to the effluent treatment plant. The tank comprised of a reinforced concrete box structure with 90 m x 35 m internal dimensions and 7.3 m internal depth. The tank was divided into two chambers, each 45 m x 35 m in size by means of a reinforced concrete partition wall. The thickness of the side wall is 0.8 m and the thickness of partition wall is 0.9 m. The foundation of the tank is in the form of 1.0 m thick raft

Submitted: 21 June 2016; Published: 30 November 2017

Reference: Shirode, N.P., Birid, K.C., Gandhi, S.R. and Nair, R. (2017). *Uplift of an Underground Tank in Northern Malabar Region, India*. International Journal of Geoengineering Case Histories, <http://www.geocasehistoriesjournal.org>, Vol.4, Issue 2, p.134-146. doi: 10.4417/IJGCH-04-02-04

foundation with 20 mm diameter bars at 150 mm centre to centre distance in both directions at the top and bottom of raft slab. The construction of the bottom raft and all the four side walls up to full height of 7.3 m was completed and the construction of top slab was underway when the failure took place.

GEOLOGICAL SETTING OF REGION

The broader region under consideration comprises of sand blankets, loamy soil, and transported lateritic red soil, that are of Pleistocene to Holocene in age. The geology of the area is characterized by hard laterite and granite in hilly tracts. Laterite is a distinctive geological formation. It has a peculiar nodular, non-homogeneous structure, cemented with ferruginous / aluminous binder, which was formed as the product of tropical weathering usually capping the rocky hills. The topography is a highly undulating hilly terrain with complex, non-uniform combination of laterite and granite rocks, overlain by sand and lateritic soil with varying thicknesses at different locations. There are areas where some of the foundations are laid by excavating the soil and some rest on filled up soil.

Based on the geotechnical investigation, which was carried out before the land grading (cutting and filling), the following subsurface stratification was observed near the tank location.

Table 1. Subsurface stratification.

Layer numbers	Depth (m)	Stratification
I	0.0-2.0	Brownish silty fine to medium sand with traces of gravels
II	2.0-6.0	Greyish yellow fine to medium sandy silt
III	6.0-7.5	Yellowish grey weathered granite rock
IV	7.5-10.0	Greyish hard granite rock

The overall topography of the project site was sloping from west towards the east. The profile of bedrock was also dipping down from west towards the east as shown with varying reduced levels (RL) in Fig. 1 along with the relative location of the tank.

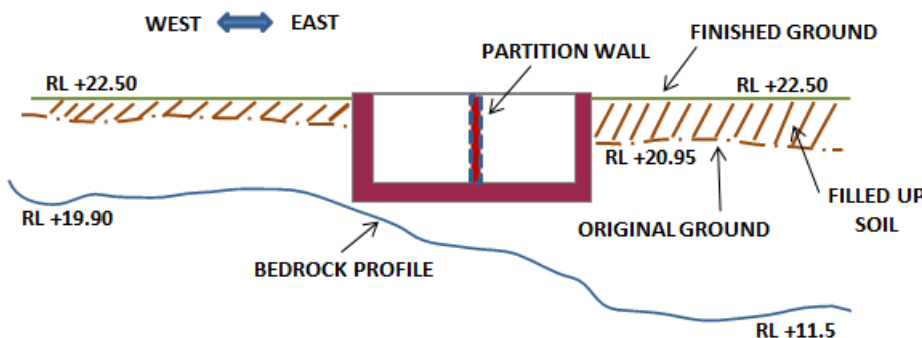


Figure 1. Topographic features near the tank.

TANK UPLIFTING AND FAILURE PATTERN

In the southern part of India, the monsoon is at its peak in the months of June & July every year. In mid-June of 2013, the foundation raft of the tank suddenly got uplifted by approximately 300 mm at the center. The review of past rainfall data revealed higher rainfall intensity in June 2013 compared to rainfall in the previous three years as shown in Table 2. During the failure of the tank, the 0.9 m thick reinforced cement concrete (RCC) partition wall inside the tank got cracked in tension at the center due to the uplifting and bending of the foundation raft. However, no uplifting was noticed at the four edges of the tank. Thus, the tank took an inverse saucer shape due to the uplifting at the center.

Table 2. Rainfall data.

Month & year	Average daily rainfall (mm)	Maximum rainfall in a single day (mm)
June 2010	28.9	114.4
June 2011	29.3	120.2
June 2012	32.3	130.2
June 2013	46.9	162.0

Fig 2 indicates the curved and cracked partition wall due to the tank uplifting. Several other cracks were observed along the height of the partition wall on either side of the middle 300 mm wide crack, with the crack width decreasing away from the center. Based on daily measurements taken on top of the partition wall after the failure, the uplifting of bottom slab and the crack width of partition wall was observed to be increasing at a rate of 30 mm per day. The cracks, which were observed on top of the foundation raft inside the tank, had maximum width of 12 mm. The seepage of groundwater inside the tank was not observed through these cracks. Thus, the depth of cracks was limited only to the top portion and not penetrating the entire thickness of the foundation raft.

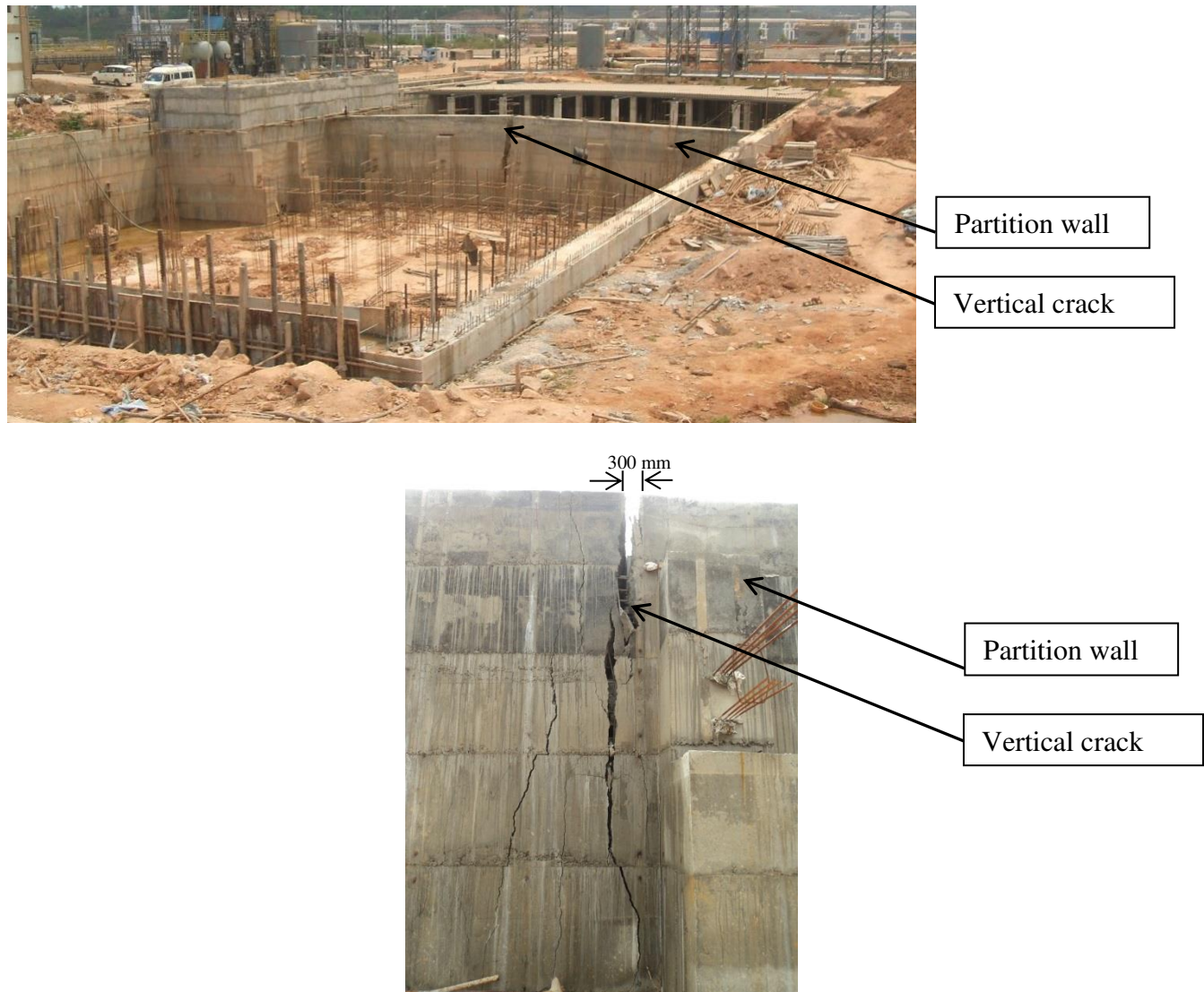


Figure 2. Uplifting and cracking of tank partition wall.

IMMEDIATE RECTIFICATION MEASURES

As the crack width in the partition wall was increasing at a rate of 30 mm per day, it was necessary to take immediate corrective measures to stop the cracks from further widening. It was therefore suggested to drill boreholes of 200 mm diameter up to 8 m depth (as the depth of tank is 7.3 m) around the tank periphery so as to reduce the water pressure acting on the bottom of foundation raft by allowing the water under pressure to get released through these boreholes. However, due to the heavy rains, the contractor could not position the drilling equipment near the tank to drill the boreholes. Considering the practical delays in carrying out the borehole activity, another suggested option was to fill the tank with water up to approximately 5.5 m height which would generate additional weight within the tank, to counter the upward buoyant force of groundwater. Thus the accumulated water within the surrounding area was diverted inside the tank. As soon as the tank started filling with water, the settlement of the tank started taking place due to the weight of water. It took more than a month to fill the tank with water up to a height of 5.50 m after which the tank was observed to be completely settled to its original position and the crack width in the partition wall was reduced to 25 mm from 300 mm.

In the meantime, when the tank filling was ongoing and the rainfall intensity reduced, the boreholes with steel liner were drilled along the tank periphery and a 1.2 m diameter and 4 m deep ring well was also dug near the tank. The groundwater was observed to be coming out from the perforations in steel liner above the ground level due to high hydraulic head (Fig. 3a). The water level in an open well was also observed to be at the ground level (Fig. 3b).

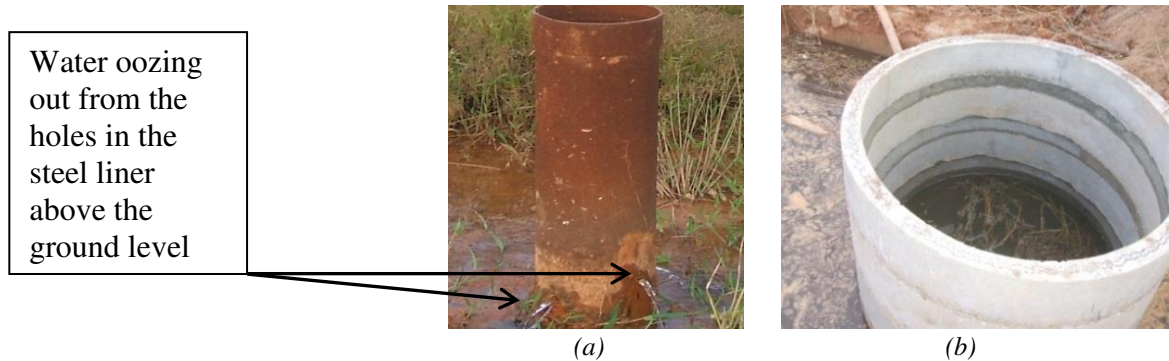


Figure 3. Groundwater level in (a) borehole with steel liner and (b) ring well

POST FAILURE INVESTIGATIONS

In order to assess the correct root cause and to design the most effective permanent rectification scheme, a detailed investigation and testing program was undertaken. The field investigation comprised of conducting hydrogeological survey and geotechnical investigations using ground penetration radar, seismic refraction test, infiltrometer test and core-cutter test to understand the subsurface profile beneath the tank foundation and in surrounding areas.

Seismic Refraction (SR)

SR survey was carried out to determine the wave propagation velocities through various soil layers around the tank and to obtain the thickness and stiffness of each layer. The seismic refraction method is based on the generation of direct compression wave (P-wave) generated using a near-surface impulsive energy that propagates through the soil media and is refracted along the boundaries of different layers. A typical test set up for SR survey is shown in Fig. 4.

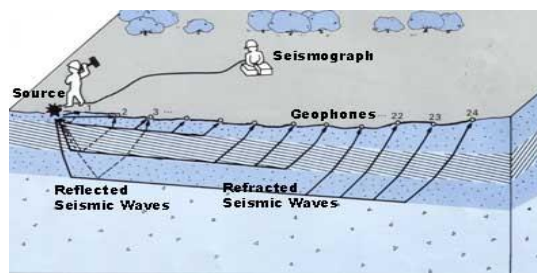


Figure 4. Typical set up for seismic refraction survey.

Ground Penetrating Radar (GPR)

GPR is a non-invasive geophysical tool that uses a high-frequency radar antenna and advanced signal processing software to accurately probe underground structures, voids and objects. Use of GPR and its applications have been discussed by Seliga et al. (2003), Davis et al. (1989), Greaves et al. (1996), Huisman et al. (2003) and Neal (2004). The prime focus of investigation was to identify the loose pockets in the subsurface, to identify the depth and dimension of subsurface anomalies, and to perform velocity analysis to elucidate the subsurface features at the survey locations.

Infiltrometer Test

The infiltrometer test was performed to measure the in-situ infiltration rate of soil. A twin ring setup is used for this purpose. A confined area was created by a steel ring of 300 mm diameter. The outer ring diameter, which is twice the inner ring diameter, is used to create the boundary condition. The time period was recorded for a specific flow of water through a known area where the flow is vertically downward.

Core Cutter Test

The core-cutter test consists of driving a core-cutter of known volume into the soil after placing it on a clean surface. The in-situ unit weight and moisture content were determined as per Indian standards IS: 2720 (Part-29) and IS:2720 (Part-2) respectively.

The numbers and tentative locations of GPR, SR tests and other field tests, with respect to the tank location, are indicated in Fig. 5 and Table 2.

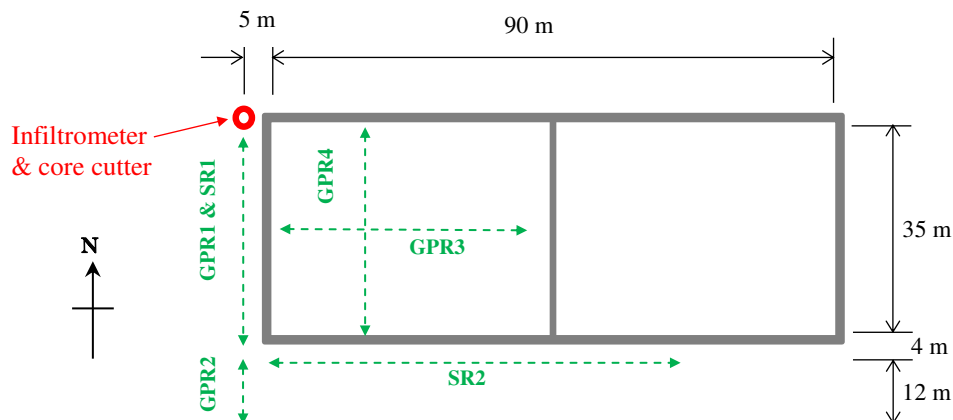


Figure 5. The schematic plan illustrating the location of GPR profiles, seismic refraction (SR) survey profiles and soil samples (see also Table 2).

Table 2. Field test location and profile details.

Locations of data acquisition	Quantity of GPR profiles collected (2D & 3D)	Quantity of seismic profiles	Type & Qty. of geotechnical sampling
West of tank	2D – 5	1	Infiltrometer- 1 & Core cutter-1
Between well and tank	2D – 23; 3D- 1	1	Test not done
Inside the tank (N-S direction)	2D - 18		Test not done
Inside the tank (E-W direction)	2D - 6		

The investigation was focused on the west and south periphery of the tank, where the ground was submerged. It shall also be noted that historically there was a perennial water well near the southwest corner of the tank which was filled up with soil and boulders during construction. The water from this well was used for household purposes by the local villagers. The concrete slab was also cast on top of this well during construction. The area on north and east of the tank was observed to be relatively dry.

Laboratory Testing

Representative disturbed and undisturbed soil samples were collected at various locations to conduct laboratory testing. The following laboratory tests were carried out on representative soil samples collected from the location around the tank as indicated in Fig. 5 and Table 2:

- Grain size distribution analysis as per IS:2720 (Part-4)
- Atterberg's limits as per IS:2720 (Part-5).
- Permeability test as per IS:2720 (Part-17)
- Collapse potential test as per ASTM D 5333

OUTCOME OF FIELD SURVEY & LABORATORY TEST RESULTS

Seismic Refraction (SR)

The seismic refraction survey data was used to classify the soil using correlations between typical velocities, type of formations and the density as suggested by Bourbie et al. (1987). Based on this classification, the top layer consists of clayey soil, which is moderately compacted up to a depth of 1.5 m with P-wave velocity of 349 m/s. It is followed by a layer of clay and gravel with a thickness of 1.5 m, having a velocity range from 377 m/s to 482 m/s and a layer of sandy silt strata up to 10 m with a thickness of about 7.5 m and a seismic velocity range from 491 m/s to 858 m/s, as shown in Fig. 6.

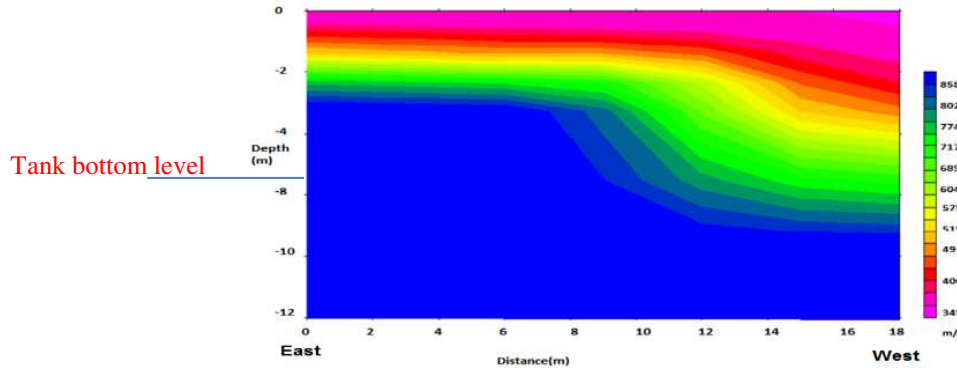


Figure 6. The soil strata profile obtained from SR2 data conducted on the south side of the tank near the closed water well (see Fig. 5 for survey location with respect to the tank).

Ground Penetrating Radar (GPR)

The key factors responsible for signal anomalies within a structure are velocity and phase inversion of electromagnetic waves. The dielectric constant of a medium determines the velocity at which the GPR signals propagate through the medium and the difference between the dielectric properties of two different materials results in reflections of electromagnetic waves. There is a direct proportionality between this difference in the dielectric properties of the contiguous media and the amount of reflected energy. The dielectric permittivity (ϵ) largely defines the propagation characteristics of radar signals. The reflection strength R is given by Equation 1 (Cassidy 2009):

$$R = (\epsilon_{r1}^{0.5} - \epsilon_{r2}^{0.5}) / (\epsilon_{r1}^{0.5} + \epsilon_{r2}^{0.5}) \quad (1)$$

where ϵ_{r1} and ϵ_{r2} are the dielectric constants of two adjacent layers 1 and 2, respectively.

Energy is radiated into the subsurface by the transmitting antenna resulting in the conical nature of the radiating beam where the center of the antenna forms the apex of the cone and the cone angle spans over a range of 60 to 90 degrees. An anomaly located in the path of the antenna results in the hyperbolic shapes in the reflection patterns. As the relative dielectric constant increases, the propagation velocity reduces and the transmission of energy into the ground becomes more focused. This forms the basis of estimation of propagation velocity through geometric scaling that involves the process of transformation of time domain GPR data to distance domain GPR data.

The distinction between the electromagnetic properties of the anomaly and the medium sets the reflectivity of the anomaly. The sensitivity of the GPR antennas increases with frequency, which in turn determines the strength of the signals reflected from the anomalies along with the reflectivity of the anomaly and the characteristic noise of the medium. High frequency GPR systems have higher resolution which is essential to distinguish between signals reflected from anomalies that are close together. In the case of fractures, the amplitude of reflections is polarized positively and has lesser strength. When the diameter of the antenna footprint at the fracture depth is less than the lateral dimensions of the fracture, it can be detected.

It shall be noted that GPR technology is based on the electro-magnetic wave propagation where the depth of wave penetration and the data resolution is affected by the geology and sub surface soil layers. If the strata is clayey, the results are susceptible to deviate from the actual. Hence it is cautioned that borehole data, if available, may be used as constraints to generate valid interpretations. Based on the output of the GPR survey the following features were identified:

South-West side of tank (Between well and tank):

Close to the side wall of the tank, the discontinuous sloping feature towards the tank at depths of 11 m to 12.5 m below existing ground level (EGL) was observed. The observed sloping feature was identified as water channel with the direction of flow from closed water well (south direction) towards the tank (north direction) as highlighted by the green line in Fig. 7.

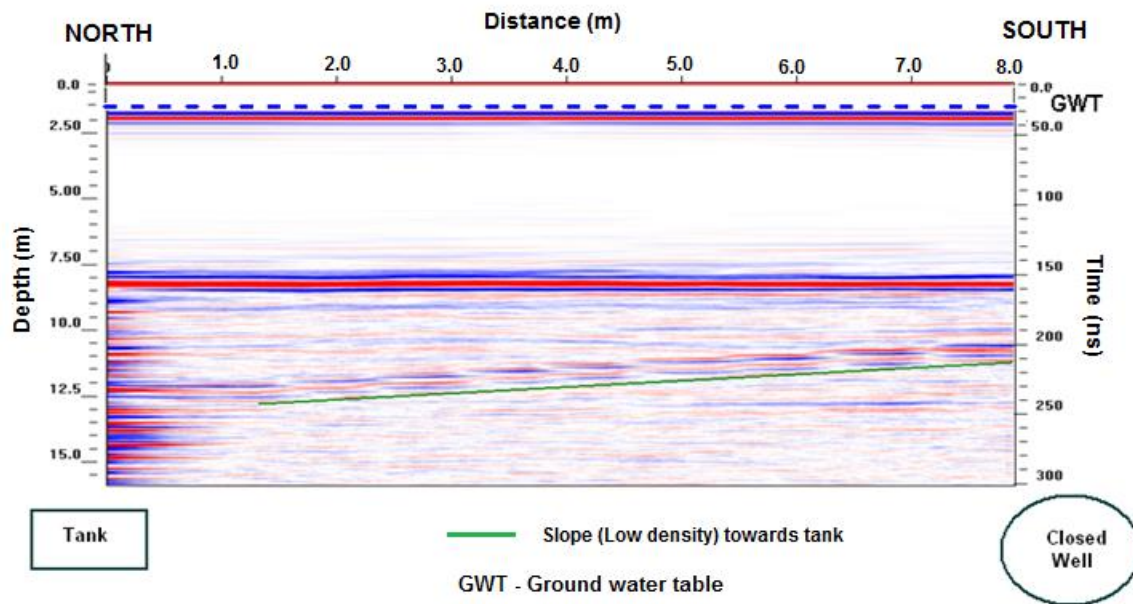


Figure 7. GPR2 profile collected using 200 MHZ antenna outside the tank along North - South direction by placing the antenna inside the floating body. This profile is located between the tank and closed water well i.e., close to the wall of tank. (see Fig. 5 for survey location with respect to the tank).

West side of the tank:

Highly saturated subsurface strata was observed near the west side of the tank at a depth of 3.5 m below the ground level. There are no visible loose pockets or other anomalous features in the subsoil strata at this location. Velocity was observed to

be decreasing with depth and the data shows six significant changes in velocities i.e., 0.27 m/ns to 0.04 m/ns with depths up to 23 m. This is because of the increase in the moisture content from 4% to 36% with increasing depth.

Beneath the tank (by carrying out survey inside the tank):

A phase inversion occurred at the concrete and void interface as indicated by a negative amplitude preceding a positive amplitude (see Fig. 8, 9 and 10). The amplitude of the GPR data is represented by red, blue and white colors. Red coloured areas represent a positive reflection and blue coloured areas represent a negative reflection while white areas represent distinct reflected areas, typically indicative of a dielectric uniformity within a given medium.

Loose pockets in the substrata were observed along the East-West direction beneath the tank bottom. The horizontal length of loose pockets below the bottom of the tank (F1 to F5) are observed to be varying between 0.5 m to 5.5 m at different locations. (see Fig. 7). The vertical thicknesses of the loose pockets are approximately 0.5 m each.

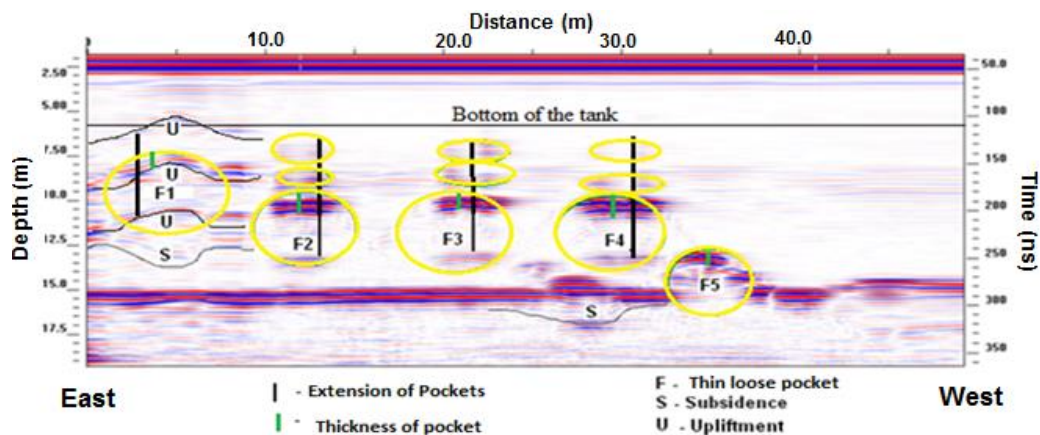


Figure 7. GPR3 profile collected using a 200 MHZ antenna inside the tank along East - West direction by placing antenna inside the floating body.

Fracture F5 is visible at the depth of 12.5 m in the profile along North-South direction (shown in Fig. 9). High amplitude reflections at 7.5 m depth are interpreted as rock formations and very high amplitude thick reflections encountered at depth of 14.5 m are interpreted as hard bedrock.

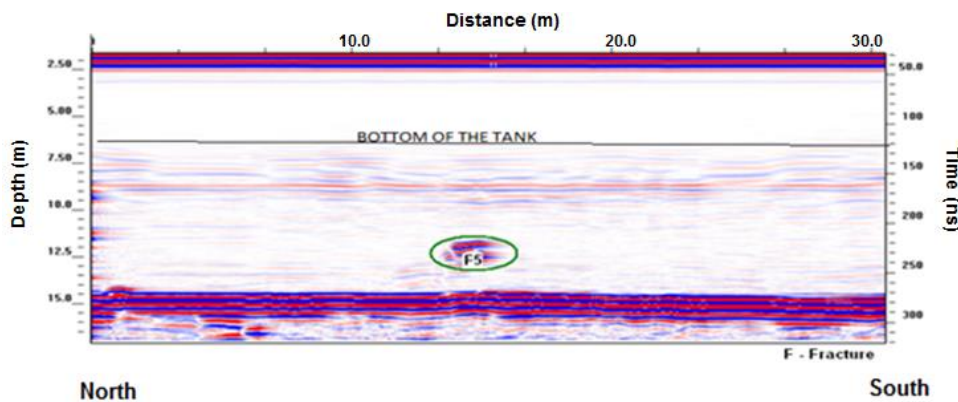


Figure 9. GPR4 profile collected using a 200 MHZ antenna inside the tank along North - South direction by placing antenna inside the floating body.

South side of tank:

3D data near the tank clearly indicates the clay rich strata at the depth of 2.5 m below ground level and the moisture is more concentrated at the depth of 7.5 m to 10 m from ground level (see Fig. 10). This visualization assisted in confirming the presence of water channels between the well and the tank.

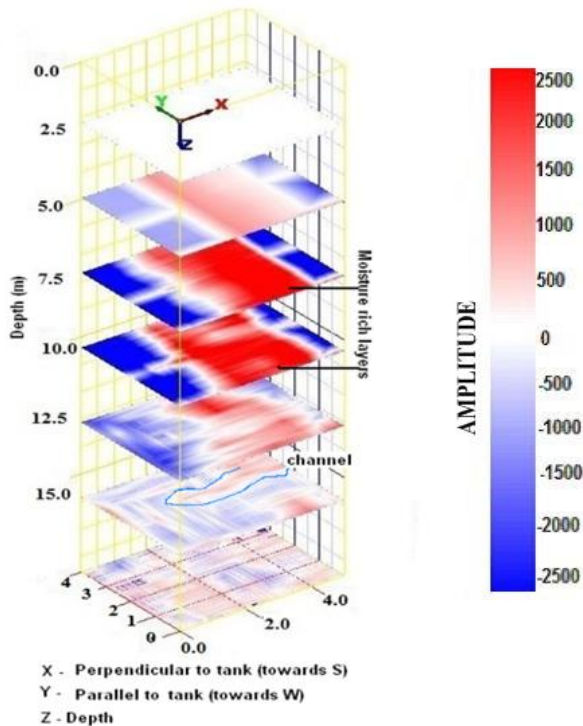


Figure 10. 3D view of the grid from GPR2 near the tank, data collected with 2 m interval at X axis and 1 m interval at Y axis. X is the direction perpendicular to the tank; Y is direction parallel to the tank and Z is the depth of penetration of the GPR2 antenna, i.e., 20 m.

Laboratory Test Results

Laboratory tests were carried out on undisturbed soil samples taken from a depth of 0.5 m below the ground level using a core cutter. The natural moisture content was observed to be 9.3% and in situ dry density of the soil was 16.66 kN/m^3 . Based on particle size analysis, the soil was classified as non-plastic Silty Sand (SM) per USCS classification. The soil was of medium permeability with coefficient of permeability of 10^{-4} cm/sec . The collapse potential of the soil was 0.016. Hence, the soil at this location was classified as “moderately trouble” per Coduto (2001). The Infiltrometer test that was performed at a depth of 0.5 m from the ground level showed a percolation rate of $8.77 \times 10^{-4} \text{ cm/sec}$ and the soil at this location was classified as of medium permeability.

ROOT CAUSE ANALYSIS

The soil densification is evaluated using the correlations between velocity, density and soil type as per Bourbie et al. (1987). The SR profile based on wave propagation velocities through different soil layers indicated non uniform soil thickness and the variation in stratification and elastic properties of soil along the west side of the tank. It was also inferred that loose to medium dense soil strata was present up to 7.5 m depth near the tank periphery. The field investigation using GPR clearly indicated the presence of underground water channels and the loose pockets within the stratification.

It can also be observed from the laboratory test results that the soil is silty sand with relatively high permeability. The lateritic nature of this soil is also prone to piping action under the different hydraulic gradient. This phenomenon was confirmed by

potential hydrocollapse strain measurement which classified the soil as “Moderately trouble” per Coduto (2001). Collapse is often triggered by a combination of increased stress and the addition of water leading to increased degrees of saturation. However, the collapse is most often triggered by an increase in the water content. Surface runoff and poor drainage control, groundwater recharge, etc. are the major sources responsible for the collapse. The generation of pockets beneath the tank clearly indicates the piping phenomenon that has taken place beneath the tank.

The general topography and geological features of the surrounding area indicate that the ground level elevation is increasing towards the west, further away from the tank location. The difference in elevation of the ground surface at the tank location and the surrounding areas has led to large amount of water flow from surrounding areas towards the tank during rainy season. Also as indicated in Fig. 1, the presence of the bedrock, which was dipping downward from west towards the east, has caused the water to flow from higher elevation to lower elevation i.e. from west towards the east direction along the bedrock surface.

The presence of a large water body was also noticed at a higher elevation with respect to the level of the tank, thus creating a large amount of hydraulic head. This water body was approximately 13 m above the ground level around the tank. The presence of a water body at this height can lead to percolation of water within the ground and development of water flow towards the area of lower elevation, i.e., tank and the surrounding areas. As the bedrock is present at higher elevation towards the western side (Fig. 1), the flow of water was taking place from the top of the bedrock towards the tank.

It can be evident from the results of the field investigations, laboratory testing and the overall topography that the excess hydrostatic pressure was generated beneath the bottom of the tank and uplifted the tank.

Design Considerations

During the initial geotechnical investigation, the depth of the water table was observed at 4.3 m (RL 18.20 m) below existing ground level (EGL) (RL 22.50 m). However, for design purposes, for conducting buoyancy analyses of the empty tank, the water table was conservatively considered at RL 19.30 m, which was 1.10 m above the observed water level.

Based on that water table, the maximum uplift force was calculated as shown below:

Area of the raft = 96 m x 40 m = 3840 m².

Uplift force = 3840 x 39.84 kPa = 152986 kN.

The total dead load of the tank is 212813 kN, which includes the weight of the top slab and supporting tie beams.

Hence, factor of safety is = 212813 / 152986 = 1.39, which is more than the acceptable norm of 1.2 as per IS standards, and hence considered safe.

In the present scenario when failure occurred, full dead weight is not applicable due to the partial construction of the tank. The dead weight of structure excluding the top slab and tie-in beams was 189117 kN. This has reduced the factor of safety to 1.24. This was still above the acceptable factor of 1.2. However, as observed in the field, the water level around the tank had increased by additional 3.4 m than that considered in design.

The increase in this level has added a force of: 3840 x 33.87 kPa = 130061 kN.

This has reduced the safety factor as;

reduced tank weight of 189117 kN / (130061 kN + 152986 kN) = 0.67 which is less than 1.

The above calculations demonstrate that this failure was a clear case of uplift due to buoyancy.

PERMANENT RECTIFICATION MEASURES

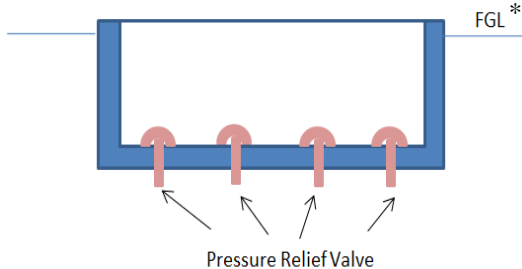
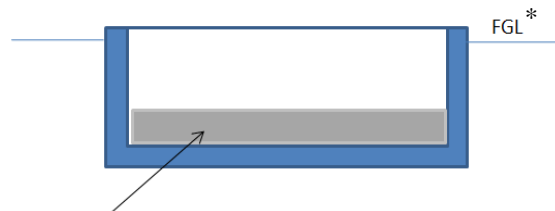
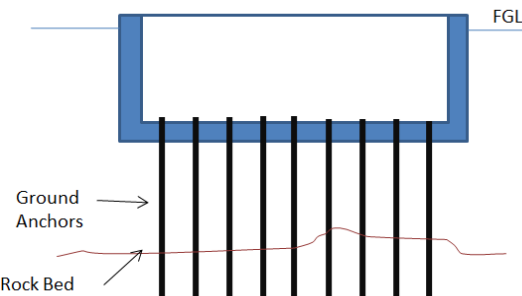
Various options were investigated as permanent rectification measures to prevent future uplifting of the tank. It was not possible to redesign the partly constructed tank to withstand the hydrostatic pressure. The options to counterbalance the buoyant force also had some limitations from a cost and schedule point of view. Hence, the cost and performance effective options to reduce the hydrostatic pressure acting on the bottom of the tank are summarized in Table 3. Based on the merits and demerits of various rectification schemes, the scheme that includes the installation of dewatering wells (option 2) all around the tank was implemented.

Thus, twelve 500 mm diameter and 20 m deep dewatering wells with perforated pipe inside were installed around the tank. Seven dewatering wells were installed along the west edge of the tank where the groundwater flow was observed to be higher. Remaining wells were installed near the north and east face of the tank. All the dewatering wells were initially installed with

2 HP submersible pumps to pump out the water continuously. The pumps had an actuator which could automatically start the pump when the water level reaches 2.5 m below the bottom of the tank and stop when the water level reaches 8.7 m below the bottom of the tank. Based on initial trials and observations, it was observed that three pumps near the south-west face of the tank used to run uninterrupted, indicating a large inflow of water at that location. This observation necessitated the increase in pump capacity from 2 HP to 5 HP. Continuous observations for some period confirmed the adequacy of numbers and capacities of pumps to cater the groundwater inflow.

Table 3. Investigated options for permanent rectification.

Options	Description	Schematic Representation	Remarks
Option 1	<p>TRENCH DRAINS:</p> <p>Intercepting drains consist of shallow trenches with collector pipes surrounded by drainage material, placed to intercept seepage moving horizontally in an upper pervious stratum. The water is pumped out from the sump tank.</p>		<p>The shallow depth of the trench may not work effectively to release the entire hydrostatic pressure from founding depth of the tank which was 7.3 m deep.</p>
Option 2	<p>DEWATERING WELLS:</p> <p>These wells are constructed by drilling a hole of sufficient diameter to accommodate a pipe column and filter and placing filter material in the annular space. The water will be directly pumped out from these wells to lower the groundwater table.</p>		<p>The provision of dewatering wells would draw groundwater from deeper depths below the foundation raft of the tank, thus reducing the hydrostatic pressure beneath the raft. The cost involved is not very high.</p>

Option 3	NON-RETURN PRESSURE RELIEF VALVES: Provision of non-return pressure relief valves on the bottom slab to release groundwater pressure, by allowing the groundwater to enter the tank through these valves.		There is a chance of groundwater contamination in case of malfunctioning of the non-return valve. This was not acceptable from an operation point of view.
Option 4	DEAD WEIGHT: Provision of dead weight in terms of 1.2 m thick layer of plain cement concrete (PCC) on top of the foundation raft inside the tank. This would increase the dead weight of the tank and would counterbalance the uplifting due to groundwater pressure.		Provision of PCC would also reduce the volume and ultimate capacity of the tank which was not acceptable from an operation point of view. Very high cost involved in this option.
Option 5	GROUND ANCHORS: Provision of ground anchors to hold the tank against uplifting.		During execution of ground anchors from inside the tank, dewatering of tank is required and has a risk of tank uplifting and cracking after dewatering. Else the groundwater level has to be temporarily lowered during anchoring by means of a well point system. Very high cost involved in this option.

* FGL - Finished Ground Level

While the peripheral dewatering wells were in continuous operation, the tank was emptied to conduct the structural repairing work. The gaps under the base slab which were formed by the tank uplift were filled with cement grout. The surface cracks developed within the base raft were also treated using epoxy bonding agent and cement grout.

The structural rectification of damaged partition wall was carried out by demolishing the damaged portion, providing new reinforcement, applying epoxy bonding coating on old concrete and reconstructing the demolished portion of the wall.



CONCLUSIONS

The original topographic features of the site play a vital role in the design of underground structures. The effect of groundwater table and subsoil stratification needs to be thoroughly investigated beforehand. Proper hydrogeological survey and geotechnical investigations needs to be planned in a complex geological region with undulating topography to avoid post construction distresses and additional cost and schedule impact after the failure.

The damage observed in this case study was mainly due to the additional hydrostatic force from the groundwater. Such problems related to groundwater pressure can be successfully resolved by allowing the water to flow freely instead of blocking its flow path. It was necessary to implement suitable structural strengthening in combination with geotechnical solutions to tackle the existing failure and prevent future failures. The underground tank presented in this case study has been in operation since the end of 2014 without any uplifting during the monsoon.

ACKNOWLEDGMENT

We are thankful to Mr. Shanker Krishna, Doctoral Student, Department of Ocean Engineering, IIT Madras, India for his assistance in analysis of GPR and SR data.

REFERENCES

ASTM International (2009). *Standard test method for infiltration rate of soils in field using double-ring infiltrometer (ASTM D3358)*.

ASTM International (2010). *Standard test method for measurement of collapse potential of soil (ASTM D5333)*.

Bourbie, T., Coussy, O., and Zinszner, B. (1987). *Acoustics of porous media*, Institute Francais du Petrole Publications, Gulf Publishing Company, Houston.

Cassidy, N. J. (2009). "Ground penetrating radar data. Processing, modelling and analysis." *Ground Penetrating Radar: Theory and Applications*, 141-176.

Coduto, D. P. (2001). *Foundation design: Principles and practices*, 2nd Ed., Prentice Hall, Upper Saddle River, New Jersey, 883.

Davis, J. L., and Annan, A. P. (1989). "Ground-penetrating radar for high-resolution mapping of soil and rock stratigraphy." *Geophysical Prospecting*, 37(5), 531–551.

Greaves, R. J., Lesmes, D. P., Lee J. M., and Toksoz, M. N. (1996). "Velocity variations and water content estimated from multi offset ground penetrating radar." *Geophysics*, 61(3), 683–695.

Huisman, J. A., Hubbard, S. S., Redman, J. D., and Annan, A. P. (2003). "Measuring soil water content with ground penetrating radar: A review." *Vadose Zone J.*, 2(4), 476–491.

Bureau of Indian Standards (1979). *Methods of test for soils: Determination of water content, Second Revision, (IS:2720-Part 2)*.

Bureau of Indian Standards (1985). *Methods of test for soils: Grain size analysis, Second Revision, (IS:2720-Part 4)*.

Bureau of Indian Standards (1985). *Methods of test for soils: Determination of liquid and plastic limit, Second Revision, (IS:2720-Part 5)*.

Bureau of Indian Standards (1986). *Methods of test for soils: Laboratory determination of permeability, First Revision, (IS:2720-Part 17)*.

Bureau of Indian Standards (1975). *Methods of test for soils: Determination of dry density of soils in-place by the core cutter method, First Revision, (IS:2720-Part 29)*.

Neal, A. (2004). "Ground penetrating radar and its use in sedimentology: Principles, problems and progress." *Earth Sci. Rev.*, 66(3–4), 261–330.

Selig, E. T., Hyslip, J. P., Olhoeft, G. R., and Smith, S., (2003). "Ground penetrating radar for track substructure condition assessment." *Proc., Implementation of Heavy Haul Technology for Network Efficiency*, Dallas, TX, 6.27-6.33.



INTERNATIONAL JOURNAL OF
**GEOENGINEERING
CASE HISTORIES**

*The Journal's Open Access Mission is
generously supported by the following Organizations:*



Geosyntec
consultants

engineers | scientists | innovators

CONETEC



ENGEO
Expect Excellence

Access the content of the ISSMGE International Journal of Geoengineering Case Histories at:
<https://www.geocasehistoriesjournal.org>